

## Liquid Helium up to 160 bar

F. Werner, G. Beaume, A. Hobeika, S. Nascimbène,  
C. Herrmann, F. Caupin, and S. Balibar\*

*Laboratoire de Physique Statistique de l'École Normale Supérieure, associé aux Universités  
Paris 6 et 7 et au CNRS, 24 Rue Lhomond, 75231 Paris Cedex 05, France*

\* E-mail: balibar@lps.ens.fr

(Received December 19, 2003; revised April 10, 2004)

*We have used an acoustic technique to pressurize liquid helium 4 up to  $163 \pm 20$  bar. This is far above the liquid–solid equilibrium pressure  $P_m$ , which is 25.3 bar in the low, temperature domain, where the experiment was performed ( $0.05 \text{ K} < T < 1 \text{ K}$ ). This is also far above 65 bar, the prediction of the standard theory for homogeneous nucleation of solid helium. However, no solidification was observed. We discuss our experimental method and the metastability of liquid helium at such very large overpressures. We also propose improvements of our experiment, in order to reach a possible instability limit of liquid helium 4 around 200 bar.*

**KEY WORDS:** Nucleation; liquid helium; solid helium; crystallization; cavitation; spinodal limit; acoustic waves.

### 1. INTRODUCTION

How far can one pressurize a liquid before it crystallizes? Superfluid helium offers a unique opportunity to consider this question. As shown by our previous studies,<sup>1–3</sup> solid helium nucleates easily from liquid helium if pressurized in the presence of walls. However, if the influence of walls is removed, the nucleation of helium crystals has to be “homogeneous”, i.e. an intrinsic property of helium, and it requires a large overpressure. In this article, we show that homogeneous nucleation of solid helium does not occur up to  $163 \pm 20$  bar, at least on a time scale of order 100 ns, the typical experimental time in our experiment; our results mean that helium can stay in a metastable liquid state in a much larger pressure range than previously thought.

In order to pressurize liquid helium far above its equilibrium pressure, we have focused high-intensity ultrasound bursts in bulk liquid helium,

away from any wall. The static pressure  $P_{\text{stat}}$  in the experimental cell was close to 25 bar, and the positive swings of the waves were as large as 140 bar. This amplitude was far more than necessary to produce cavitation in the negative swings of the wave. The calibration of the wave amplitude was obtained by studying the dependence of the cavitation threshold on the static pressure in the cell, as explained in a previous publication.<sup>4</sup>

When reaching 163 bar, we have achieved a much larger overpressure than ever done before. If liquid helium is compressed in ordinary cells, “heterogeneous” nucleation of helium crystals occurs a few millibars only above the liquid–solid equilibrium pressure  $P_m = 25.3$  bar.<sup>5</sup> Balibar *et al.*<sup>1</sup> suggested that this was due to the presence of graphite dust particles in ordinary cells. On a clean glass plate, Chavanne *et al.*<sup>2,3</sup> found that nucleation of crystals occurred 4.3 bar above  $P_m$  and showed that it took place on one particular defect at the surface of the glass. After removing the glass plate from Chavanne’s setup, we expected this nucleation to occur near 65 bar, the prediction from the standard homogeneous nucleation theory.<sup>6</sup> Our results show that the standard theory fails to predict the nucleation pressure of solid helium.

In this article, we first present experimental techniques, including the calibration method from an analysis of cavitation (Section 2). In Section 3 we describe our search for the nucleation of crystals. At the end of this article, we discuss possible reasons why the standard nucleation theory fails. We also discuss the possible existence of an instability around 200 bar,<sup>7</sup> and how we could reach it. In fact, our experiments explore a new region in the phase diagram where the properties of metastable liquid helium are rather unknown. Of particular interest is the pressure variation of its superfluid transition temperature.

## 2. EXPERIMENTAL METHOD

The present results were obtained with an experimental setup similar to the one previously used by Chavanne *et al.*<sup>2,3</sup> We have focused bursts of 1 MHz acoustic waves and studied the possible nucleation of bubbles or crystals by shining laser light through the acoustic focal region (see Fig. 1), a technique which was first introduced by Nissen *et al.*<sup>8</sup> The sound emitter was the same hemispherical piezoelectric transducer as in Refs. 2 and 3. In Refs. 2 and 3, the transducer was pressed against a glass plate in order to measure the instantaneous density, i.e. the sound amplitude at the focus. In the course of this former study, it was verified that the size of the acoustic focal region was one acoustic wavelength, 0.36 mm in liquid helium at  $P_m = 25.3$  bar. The threshold pressure for the nucleation of helium crystals was found to be  $P = P_m + 4.3$  bar. When the pres-

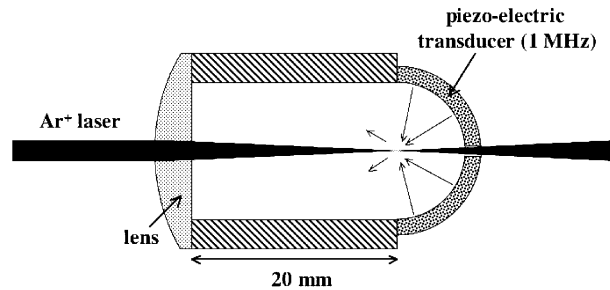


Fig. 1. The present experimental setup is only slightly modified with respect to the one used by Chavanne *et al.*<sup>3</sup>. A hemispherical piezoelectric transducer emits and focuses bursts of ultrasound at its center. A green Ar<sup>+</sup> laser is used to detect the possible nucleation of bubbles by the negative swings or crystals by the positive swings at the acoustic focus.

sure exceeded this pressure during the positive swings of the acoustic wave, crystals grew with a large velocity before melting during the following negative swing.<sup>9</sup> The observed growth velocity was a significant fraction of the sound velocity, so that crystals could grow up to several microns in times of order 100 ns, a fraction of the sound period. The details of the growth and melting mechanisms were not fully understood,<sup>9</sup> but the ability of helium crystals to grow very fast from superfluid helium at low enough temperature is well known.<sup>10-12</sup>

Chavanne *et al.* showed that the light scattering technique was a fast detection method, sensitive enough to detect crystals of micrometer size, not only bubbles.<sup>3</sup> As compared to the experiments by Caupin *et al.*,<sup>4</sup> Chavanne's detection sensitivity had been improved by focusing the light at the acoustic focus with a lens *inside* the experimental cell (see Fig. 1). As done in the present work, Chavanne *et al.* detected the light transmitted through the acoustic focal region with a photomultiplier tube (PMT) whose response time was of order 100 ns. In the focal region, the high intensity acoustic wave scatters light at small angle, so that more and more light is missing in the forward direction as the acoustic amplitude is increased. Bubbles or crystallites scatter light more strongly and at larger angle. In order to detect nucleation, one could measure either a decrease in the intensity of light along the optical axis in the forward direction or an increase in light intensity a few degrees away from this axis (see Fig. 2). Some nucleation events were detected with a larger signal to noise ratio away from the axis, but detecting in the forward direction guaranteed that no nucleation event was missed. A clear signature of the sound amplitude reaching a nucleation threshold was the observation of a random change to a different shape of the scattered light amplitude.<sup>4</sup> This is because the

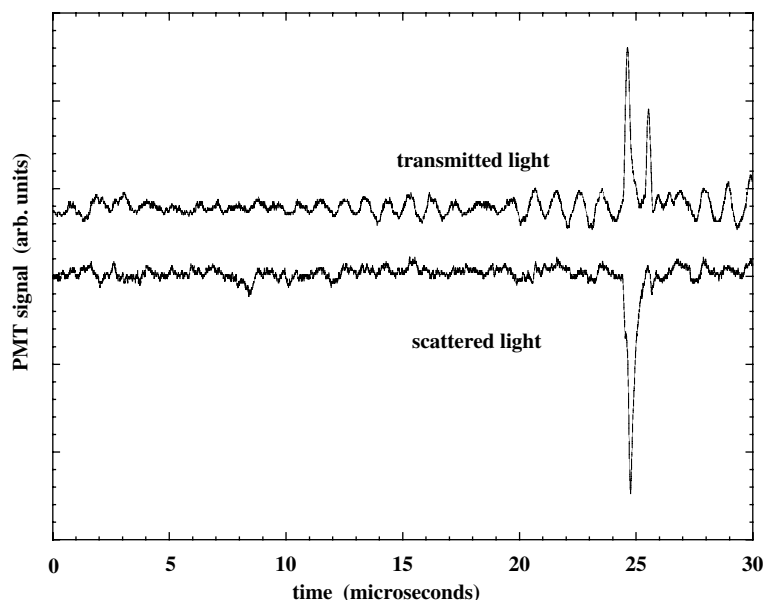


Fig. 2. Two recordings showing the detection of acoustic cavitation in liquid helium at 25 bar and 55mK. A photomultiplier tube (PMT) detects either a decrease in the light transmitted through the acoustic focus or an increase of the light scattered by the bubbles away from the optical axis.

nucleation itself is a random process; the threshold is defined by the sound amplitude which corresponds to a cavitation probability of one-half.

Knowing that, if present, crystals were easy to detect with this setup, we removed Chavanne's glass plate and tried to increase the amplitude of the sound wave as much as possible, looking for the homogeneous nucleation threshold. We started by exciting the transducer at its resonance frequency in its fundamental thickness mode (1.013 MHz). We used bursts of 3–6 oscillations with a repetition rate of 1–5 Hz. For their amplification, we first used a linear amplifier (see Fig. 4), which delivered a voltage amplitude up to 70 V on  $50 \Omega$ ; the envelope of the bursts was square (see Fig. 3) and the stability was very good (0.1% over several hours, thanks to a temperature regulation of the box containing it). We then used a tuned amplifier which was more powerful (up to 265 V amplitude) but which had less stability and some distortion of the burst envelope (Fig. 5).

The upper trace in Fig. 3 shows the excitation voltage applied to the transducer when using the linear amplifier. The lower trace shows a typical signal detected by the PMT when the applied voltage exceeded the cav-

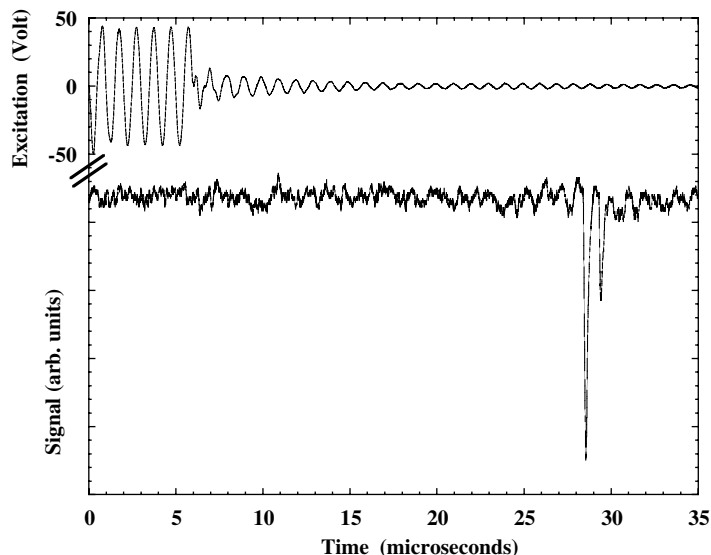


Fig. 3. The upper trace is a recording of the voltage applied to the transducer. It is a burst of six oscillations at 1.013 MHz, the resonance frequency in the thickness mode. The lower trace shows the amplitude of the scattered light detected by the PMT. The delay of the cavitation event is due to the flight time of the sound wave from the transducer surface to the acoustic focus. We have carefully analyzed this delay (see text).

itation threshold. In this particular case, the PMT was located off axis so as to detect the light scattered at large angle by the bubbles. The delay between the excitation and the detection corresponds to the flight time of the acoustic wave from the transducer wall to the acoustic focus. This is an important quantity which is further discussed below.

How did we know that this nucleation event was a bubble, not a crystal? Mainly from a study of the nucleation threshold voltage  $V_c$  as a function of the static pressure  $P_{\text{stat}}$  in the cell. As we decreased  $P_{\text{stat}}$ ,  $V_c$  also decreased (see Fig. 6). This behavior was of course consistent with nucleation of bubbles, which had to be easier at lower pressure. On the contrary, the nucleation threshold for crystals would have increased.

In the linear approximation, the sound amplitude at the acoustic focus is given by:

$$\Delta P = P - P_{\text{stat}} = R \omega^2 \rho_L \zeta, \quad (1)$$

where  $R$  is the inner radius of the transducer,  $\omega = 2\pi f$  is the angular frequency of the wave,  $\rho_L$  is the density of the liquid, and  $\zeta$  is the amplitude of the displacement at the inner surface of the transducer.<sup>4</sup> Since  $\zeta$  is pro-

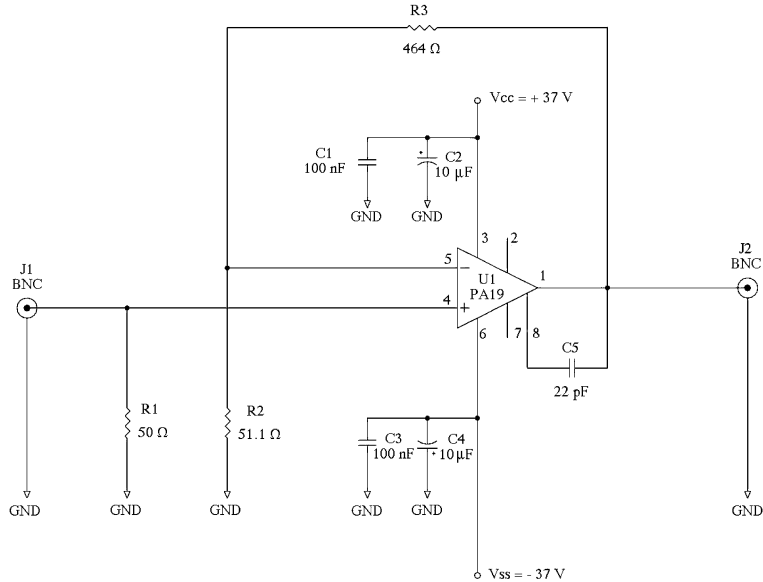


Fig. 4. The electronics of the linear amplifier. It uses a PA19 amplifier from APEX and delivers up to 70 V of amplitude on a 50  $\Omega$  resistor. It amplifies bursts of a few oscillations at 1 MHz with a high stability and an accurately square envelope.

portional to the voltage applied to the transducer, one expects the wave amplitude at the acoustic focus to be proportional to the product  $\rho_L V$  in this linear approximation. Since the cavitation pressure is constant, one then expects the threshold amplitude  $\rho_L V_c$  to vary linearly with the static pressure  $P_{\text{stat}}$ , and this is indeed what is shown by Fig. 6. Caupin and Balibar<sup>4</sup> had already noticed that non-linear effects are small in the case of hemispherical transducers, while Chavanne *et al.*<sup>14</sup> and Appert *et al.*<sup>15</sup> have shown that they are large in a fully spherical geometry. We have not yet found a robust interpretation for this difference. However, in the spherical geometry, the fluid velocity has to be zero at the center, by symmetry, while in the hemispherical geometry there is no such constraint. Although we suggest that this is the origin of the difference in behavior, our possible interpretation would need to be supported by a calculation of the exact pressure field at the center in the hemispherical geometry, but this difficult calculation has not yet been done.

With a few measurements in the small pressure range  $0 < P_{\text{stat}} < 1.4$  bar, Caupin and Balibar<sup>4</sup> had found a quasi-linear variation of  $P_{\text{stat}}$  versus  $\rho_L V_c$ , which extrapolated to  $-8$  bar at zero voltage. They explained that this had to be taken as an upper bound for the cavitation pressure,

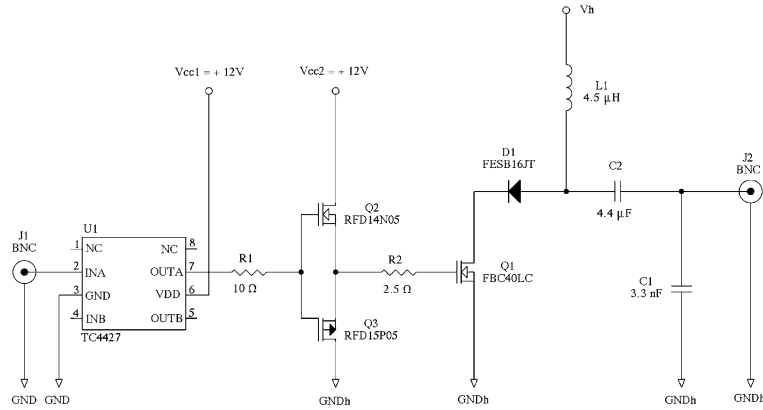


Fig. 5. The electronics of the tuned amplifier. Its design is adapted from Ref. 13. It uses two field effect transistors from Fairchild Semiconductor (RFD14N05 and RFD15P05), followed by another one from International Rectifiers (FBC40LC); dc voltages  $V_h$  from 0 to about +265 V are applied to set the output ac voltage amplitude to about the same value, 0–265 V on a 50  $\Omega$  resistor. The role of the U1-TC4427 circuit is to drive the two RFD mosfets which drive the FBC mosfet; the diode D1 allows to reverse the output voltage so that the output peak-to-peak voltage is doubled. The amplifier is tuned to 1 MHz with a bandwidth of approximately 100 kHz. The grounds GND and GNDh are connected in the power supply only.

which was predicted to be  $-9.4$  bar in the low-temperature limit. It was an upper bound because it was calculated that non-linear effects would bend the curve  $P_{\text{stat}}(\rho_L V_c)$  downwards, a consequence of the curvature of the equation of state.

Thanks to the lens which improved our sensitivity, we could now follow the acoustic cavitation up to the melting pressure at 25.3 bar, and we found a linear behavior in the much wider pressure range  $18 < P_{\text{stat}} < 25.3$  bar. Below 18 bar, since the density of liquid helium is too small, the lens focuses light too far away from the acoustic focus for a good detection. The static pressure now extrapolates to  $-9.45$  bar at zero excitation voltage, which is close to the theoretical prediction for bubble nucleation, about 0.2 bar higher than the spinodal limit at  $-9.65$  bar.<sup>4</sup> The good agreement with theory and the good linear variation provided us with a reliable calibration of our wave amplitude. For example, we concluded that, if the static pressure was 25.3 bar, exciting the transducer with a voltage  $V = 60$  V at 1.013 MHz and during three periods, produced a maximum negative swing of amplitude  $25.3 - (-9.4) = 34.7$  bar.

It is now necessary to consider the quality factor  $Q$  of the transducer. Since  $Q$  is large but finite, the response of the transducer to an excitation

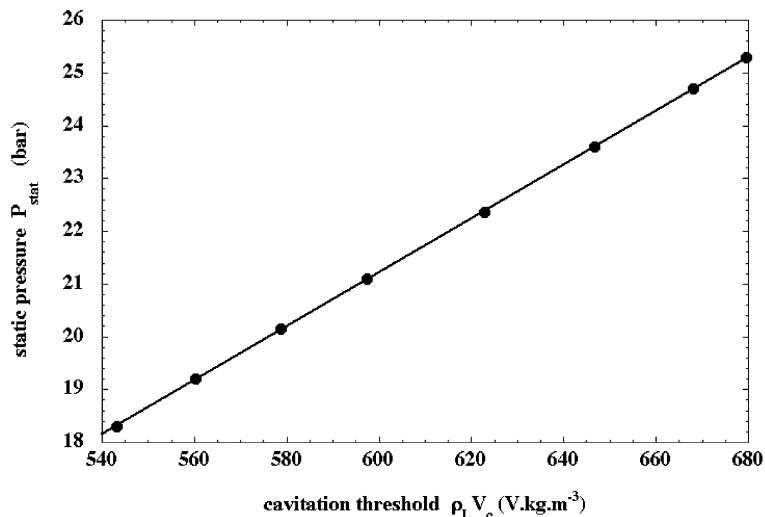


Fig. 6. The cavitation threshold varies linearly with the static pressure  $P_{stat}$  in the cell. The quantity  $\rho_L V_c$  is the product of the static liquid density by the critical excitation voltage at which the cavitation probability is one half. For this particular graph, the voltage was taken at the output of the function generator, before amplification. The linear fit extrapolates to  $-9.45$  bar where  $V_c$  would be zero. This cavitation pressure is  $0.2$  bar above the spinodal limit of liquid helium 4, in very good agreement with theoretical predictions.

voltage  $V_0 \sin(\omega t)$  starting at time  $t=0$  is<sup>16</sup>

$$\zeta(t) \simeq \frac{AV_0}{2\omega^2} [\sin(\omega t) - Q(1 - \exp(-\omega t/Q)) \cos(\omega t)]. \quad (2)$$

After the excitation stops, at time  $t = 2\pi n/\omega$ , the oscillation amplitude decreases proportionally to  $\exp(-\omega t/Q)$  (see Fig. 7). As previously done in Ref. 4, we have measured  $Q$  by studying the cavitation threshold voltage as a function of the number  $n$  of periods in the burst. The fit in Fig. 8 corresponds to  $Q = 56$ ; it was made for  $n \geq 6$  only because, given the polarity of the transducer (see below), the most negative amplitude was reached after  $n - 1/2$  periods for  $n \geq 6$ , but after  $n + 1/2$  periods if  $n < 6$ . We could choose to emit waves with two different shapes, which respectively corresponded to two symmetric configurations (see Fig. 7):

- (A) The electrical excitation starts with a negative voltage on the inner electrode of the transducer. As a result the thickness of the transducer first decreases and the liquid is locally depressed: an acoustic wave is emitted, which starts with a negative pressure

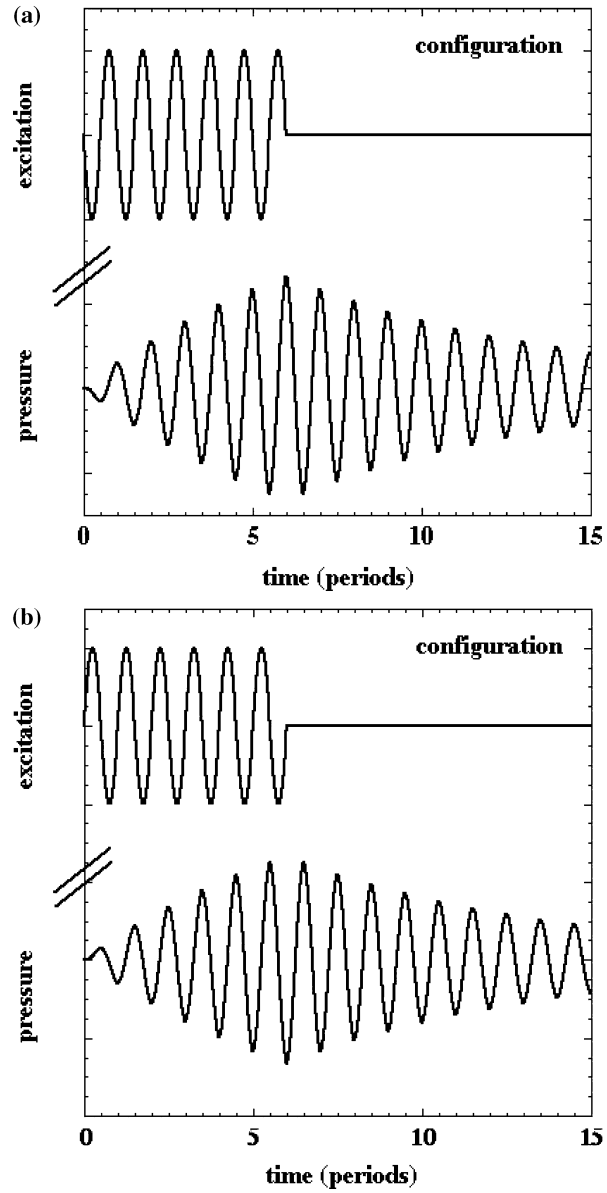


Fig. 7. The excitation voltage and the pressure emitted at the transducer surface, in the two symmetric configurations A and B. The envelope of the pressure oscillations reflects the existence of a finite quality factor  $Q$ . The two graphs are drawn with  $n=6$  and a quality factor  $Q=50$ . In this case, the most negative pressure is reached after  $n-1/2$  periods in configuration A, and after  $n$  periods in configuration B.

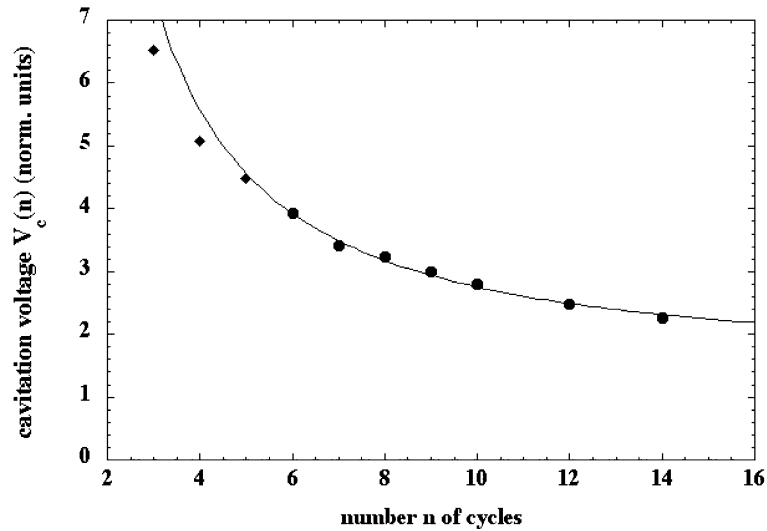


Fig. 8. We have studied the cavitation threshold voltage as a function of the number of oscillations  $n$  in the excitation burst. A fit with a simple exponential law (see text) allowed us to measure the quality factor  $Q$  of our transducer. The fit is made for  $n \geq 6$  because, only then, the most negative amplitude of the transducer oscillation is reached after  $n+1/2$  periods (see text).

swing. The most negative swing occurs  $(n - 1/2)$  periods later if  $n \geq 6$  (respectively,  $n + 1/2$  if  $n < 6$ ).

- (B) The electrical excitation is reversed, it starts with a positive voltage on the inner electrode, so that the wave starts with a positive pressure swing and the most negative swing occurs  $n$  periods later.

We have analyzed the time at which cavitation occurs, as a function of the static pressure (Fig. 9), in configuration A. For this, we needed the sound velocity which is related to the equation of state

$$P = -9.6201 + \frac{(1405.4)^2}{27}(\rho_L - 0.094262)^3 \quad (3)$$

with pressures  $P$  in bar and densities  $\rho_L$  in  $\text{g/cm}^3$ . This is the simple form proposed by Maris.<sup>17</sup> Here we adjusted it on Abraham's high pressure data,<sup>18</sup> so that the numbers are slightly different from what Caupin and Balibar obtained with a fit on low-pressure data.<sup>4</sup> The corresponding sound velocity writes:

$$c = 4685(\rho_L - 0.094262) \quad (4)$$

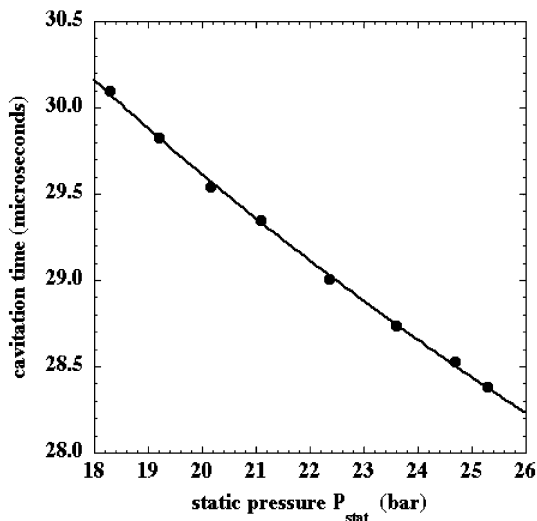


Fig. 9. A fit of the flight time as a function of the static pressure  $P_{\text{stat}}$  in configuration A. From the present fit, and knowing the equation of state (see text), we deduced that the focal distance was  $8.04 \pm 0.01$  mm, very close to the geometrical radius ( $8.00 \pm 0.05$  mm).

with  $c$  in m/s. In Fig. 9, nucleation occurs at a time  $t_n$  which is well represented by

$$t_n = (6 + 1/2)t_0 + \frac{8.04 \times 10^{-3}}{c}, \quad (5)$$

where  $t_0 = 0.987 \mu\text{s}$  is the sound period at 1.013 MHz. In this experiment, the focal distance was thus determined as  $8.04 \pm 0.01$  mm, in good agreement with the inner radius  $R = 8 \pm 0.05$  mm of our transducer. In fact, this transducer was not a perfect hemisphere: it had one hole at the pole to allow the transmission of light, plus another hole on one side in order to make the electrical connection to the inner electrode. Furthermore this connection was made with a droplet of silver paint which was covered with some epoxy glue to make it stronger. Given all these modifications of the original hemi-spherical shape, we could have found a larger difference between its radius and the focal distance.

Once we had understood the cavitation time in such details, we verified that our picture was correct by measuring the nucleation threshold on successive oscillations. We observed nucleation on earlier and earlier oscillations as we increased the excitation voltage, as shown by the recordings of Fig. 10. The lowest recording corresponds to the configuration A and an excitation voltage 59.5 V during three periods. The static pressure was

$P_{\text{stat}} = 25.0$  bar where, the sound velocity being 365 m/s, the flight time of the acoustic wave had to be  $22.02 \mu\text{s}$ . The PMT was in the forward direction and detected some modulation at 1 MHz due to the scattering by the acoustic wave, but no cavitation. The next recording corresponds to a slightly higher voltage (60 V), and random cavitation was detected at the time  $25.5 \mu\text{s}$ . This is precisely equal to  $(3+1/2)$  periods plus the flight time  $22.02 \mu\text{s}$ , as expected. When we further increased the excitation voltage to 62.5 V, cavitation occurred at time  $24.5 \mu\text{s}$  corresponding to the oscillation  $(2 + 1/2)$ . Increasing the excitation to 70 V produced cavitation on the oscillation  $(1 + 1/2)$  and a signal appeared at  $23.5 \mu\text{s}$ .

For cavitation to occur after half a period only, the voltage threshold was 265 V. The upper set of two superimposed recordings in Fig. 11 shows that cavitation was random at time  $22.5 \mu\text{s}$ : at this voltage, the signal showed cavitation with probability 0.5. This figure also shows that, when switching from configuration A to B, cavitation times are displaced by half a period: with 105 V in configuration B, cavitation occurred at  $23.0 \mu\text{s}$ , the flight time plus one period. In configuration B, cavitation occurs at lower voltages than in configuration A, because, the oscillation amplitude increases during one full period instead of half a period. Qualitatively, all these cavitation voltages (60, 62.5, 70, 265 and 105 V) are consistent with the expected shapes shown in Fig. 7, with some slight discrepancies due to the envelope of the bursts being not exactly square when using the tuned amplifier. In Section 3, we show how we pressurized liquid helium up to 110 bar in this series of measurements.

### 3. SEARCH FOR THE HOMOGENEOUS NUCLEATION THRESHOLD OF SOLID HELIUM

Within the linear approximation described in Section 2, the pressure at the focus is simply related to the excitation voltage. Of course, this is only true if cavitation has not modified the sound amplitude at earlier time. In configuration B, we observed random cavitation at time  $t = 23 \mu\text{s}$  for a voltage  $V = 105$  V (see Fig. 11). This means that the pressure was  $-9.4$  bar at that particular time. Since the static pressure was 25.0 bar, the amplitude of the negative pressure swing was 34.4 bar. With 265 V excitation in configuration A, and when cavitation did not occur at  $22.5 \mu\text{s}$ , the maximum pressure was thus  $25 + 265/105 \times 34.4 = 110$  bar. It was reached at time  $23 \mu\text{s}$ . If we supposed that non-linear effects were not negligible, our previous studies<sup>14,15</sup> showed that the positive swings would have been larger than the negative ones, so that the maximum pressure would have been even larger.

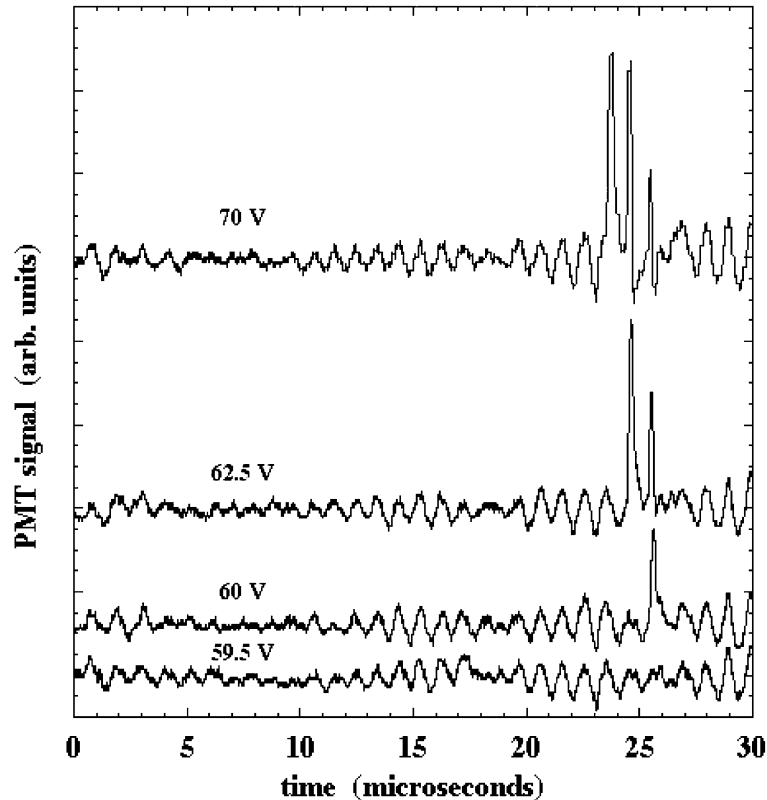


Fig. 10. Four recordings of the light intensity transmitted through the acoustic focus. For clarity, the curves have been shifted in the vertical direction. As indicated, the respective excitation voltages were 58.5, 60, 62.5, and 70 V. The burst duration was three periods at 1.013 MHz and we used the tuned amplifier. Potential 59.5 V was below the cavitation threshold voltage: only the scattering of light by the acoustic wave was detected. Potential 60 V was at the cavitation voltage at time  $25.5 \mu\text{s}$  corresponding to the oscillation number  $3 + 1/2$ . At 62.5 V, cavitation occurred on the oscillation  $2 + 1/2$  (at  $24.5 \mu\text{s}$ ) and at 70 V it occurred on the oscillation  $1 + 1/2$  (at  $23.5 \mu\text{s}$ ).

At this stage in our search, we were limited by the maximum output voltage of our RF amplifier. We pressurized liquid helium even further by using a primitive method. Instead of exciting with amplified bursts at the thickness mode frequency (1.013 MHz), we used an ordinary voltage supply and a switch (see Fig. 12). We added a few resistors and a capacitor in order to apply the high voltage only during about  $10 \mu\text{s}$ . The  $44 \Omega$  resistor in series limits the possible current in case of electrical breakdown

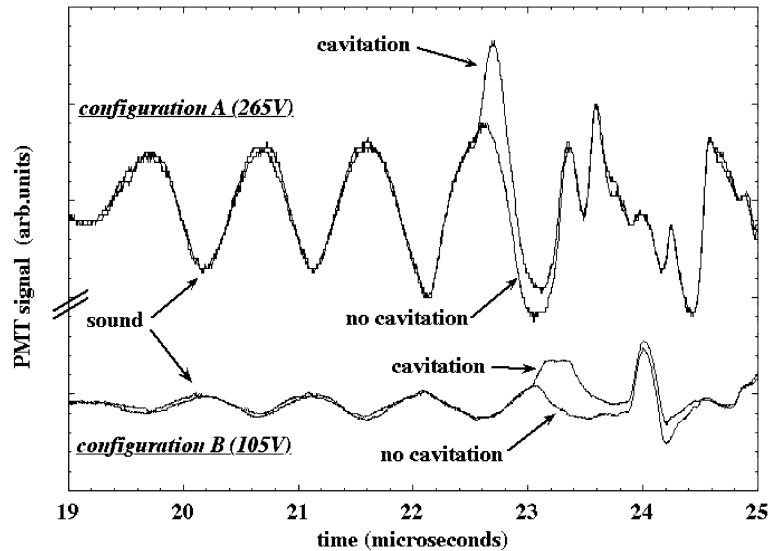


Fig. 11. These two sets of two superimposed recordings show that cavitation occurs half a sound period later in configuration B than in configuration A. This is simply because the phase of the sound wave is reversed. In each case, the voltage is adjusted at the cavitation threshold so that the detected signal shows cavitation with a probability 0.5.

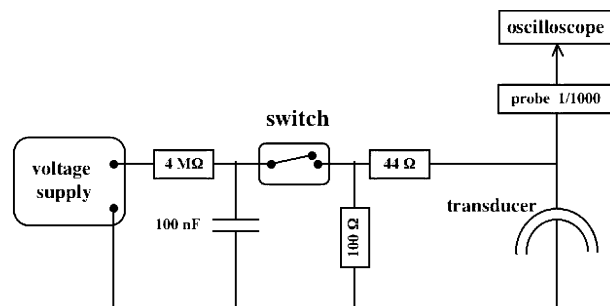


Fig. 12. It appeared possible to study cavitation and overpressurized liquid helium with this simple setup. A high voltage supply is connected to the piezoelectric transducer via a switch (a high voltage relay Meder Electronics ME12-1A69-150). Thanks to the 100 nF capacitor and the few resistors, the high voltage is applied during a time of order  $10 \mu\text{s}$  only.

somewhere along the leads to the transducer. The  $100 \Omega$  resistor allows the capacitor to discharge quickly after the switch is closed, while the  $4 \text{ M}\Omega$  resistor forces the charge of the capacitor to be slow compared to the microsecond time scale of the experiment. Fig. 13 shows the resulting voltage applied to the transducer when the voltage supply was set to 340 V.

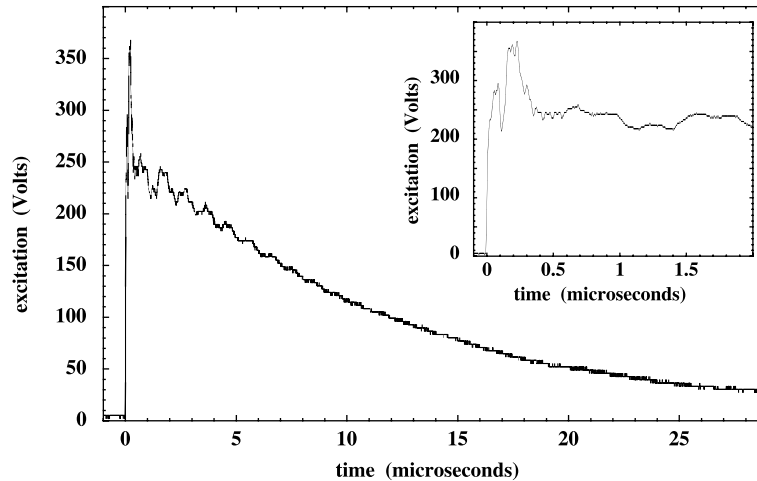


Fig. 13. The voltage on the inner side of the transducer when the voltage supply is set to +340 V in the circuit shown in the Figure. The inset shows a magnification of the recording in the time interval from 0 to 2  $\mu$ s.

With this primitive method, we were able to observe cavitation with a positive voltage  $V = +190$  V on the inner side of the transducer (configuration C). Fig. 14 shows that cavitation occurs at time 23  $\mu$ s. This is consistent with the response of the transducer to a positive step voltage, which starts as  $\zeta(t) \propto (1 - \cos(\omega t))$  and has a first minimum after one full period. A potential 190 V is the threshold voltage for this phenomenon whose random character is again shown by the superposition of two different recordings obtained with the same excitation voltage. These two recordings also show some signal as early as 22  $\mu$ s. It is due to the light scattering by the intense acoustic wave since it is reproducible, never random at 190 V. When increasing this voltage further, a random increase of the signal was observed at the new threshold voltage +340 V. This is shown in Fig. 15.

After having observed these cavitation thresholds, we reversed the voltage. As shown in Fig. 16, we observed random cavitation at 22.5  $\mu$ s for a voltage  $V = +265$  V on the outer side of the transducer, or  $-265$  V on the inner side which was equivalent (configuration D). The signal at 22  $\mu$ s was due to light scattering by the acoustic wave only, as shown in Fig. 17. This figure shows a progressive increase of the signal in the time interval 22–22.5  $\mu$ s as a function of the applied voltage. As can be seen, the signal increases continuously; no discontinuity or random change signaled any crystal nucleation. The potential 1370 V was the maximum voltage we could use, since, beyond it, sparks started to occur near the transducer.

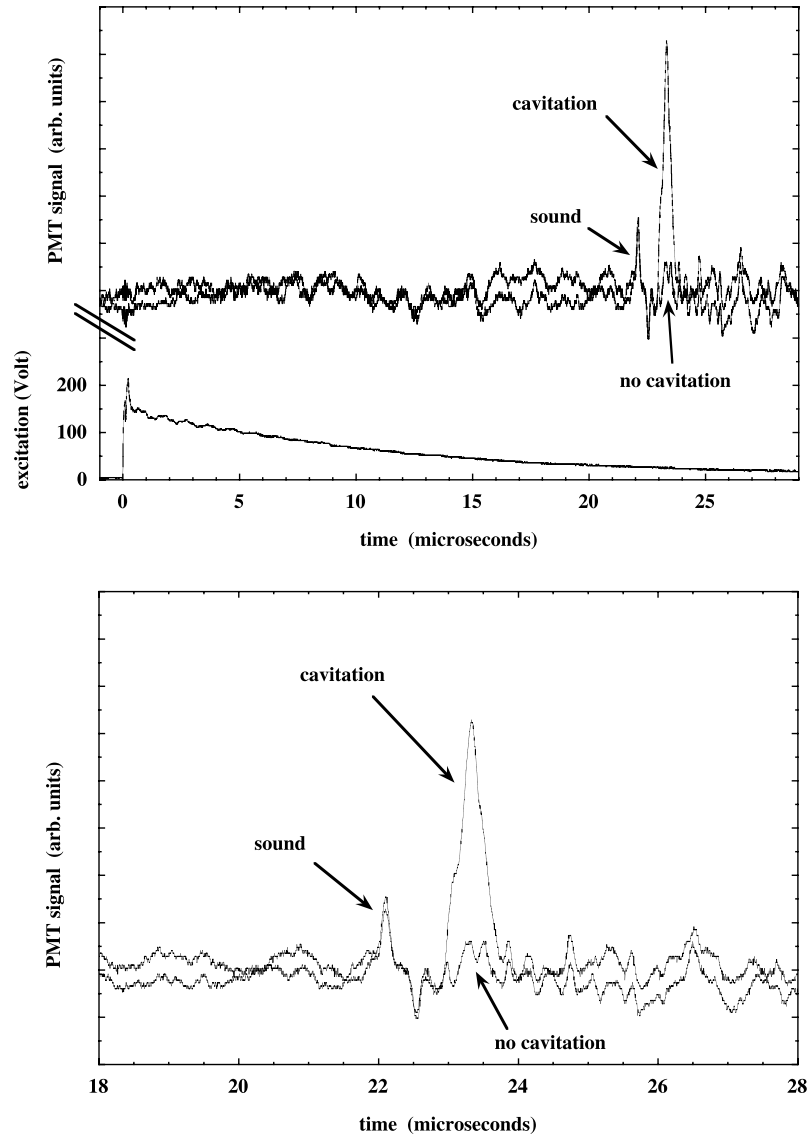


Fig. 14. The upper graph and the lower one show the same cavitation signals. The lower graph is just a magnification in the time interval from 18 to 28  $\mu\text{s}$ . In the upper graph, the lower curve is a recording of the voltage applied on the inner side of the transducer when the voltage supply is set to +190 V (configuration C). The two superimposed curves were recorded for two successive bursts with the same excitation voltage; they show that cavitation is stochastic at 190 V. It occurs at time 23  $\mu\text{s}$ , as can be seen more easily on the magnified graph below. Some light scattering from the acoustic wave is also visible at 22  $\mu\text{s}$  and later.

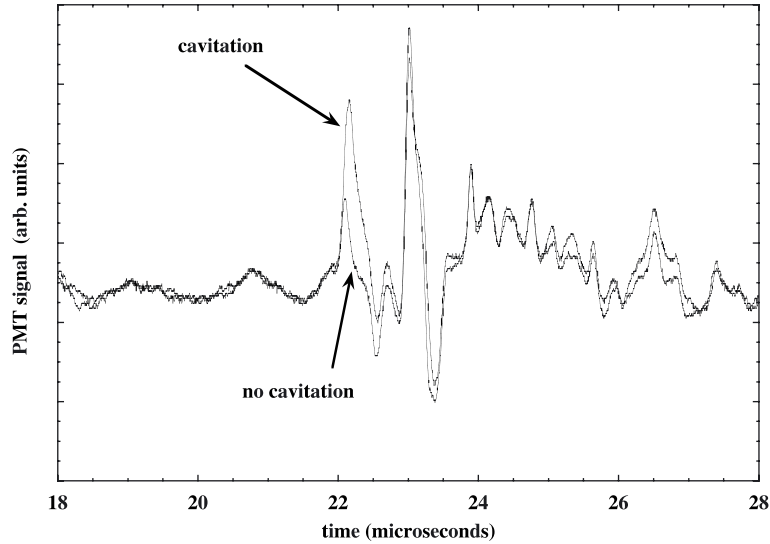


Fig. 15. For an excitation voltage  $V = +340$  V applied to the inner side of the transducer (configuration C, as in the previous figure), random nucleation of bubbles is observed at  $22 \mu\text{s}$ .

er, which progressively destroyed the connection to it. As done before, we estimated the maximum pressure reached at  $22 \mu\text{s}$  from the cavitation threshold voltage in the symmetric configuration. We obtained  $P_{\text{max}} = 25 + 34.4 \times 1370/340 = 163$  bar. The error bar on this result is  $\pm 20$  bar, mainly due to the accuracy of the pressure measurement. Since we observed no nucleation of any helium crystal, we believe that this is the highest degree of overpressurisation ever achieved in liquid helium.

The above described series of measurements was done at 55 mK. In our previous studies of cavitation<sup>4</sup> or crystallization on a glass plate,<sup>3</sup> we had observed a crossover from a quantum nucleation regime below 200 mK to a classical regime above 200 mK where, due to increasing thermal fluctuations, the nucleation threshold decreases. We thus repeated our search for homogeneous nucleation of solid helium at higher temperature. The results were similar: we observed no crystal nucleation up to 156 bar at 430 mK, nor up to 146 bar at 1.0 K.

#### 4. CRITICAL DISCUSSION

As shown in Fig. 18, our results contradict the prediction by the standard theory of homogeneous nucleation. Either this theory is too simple or we have missed the nucleation for some experimental reason.

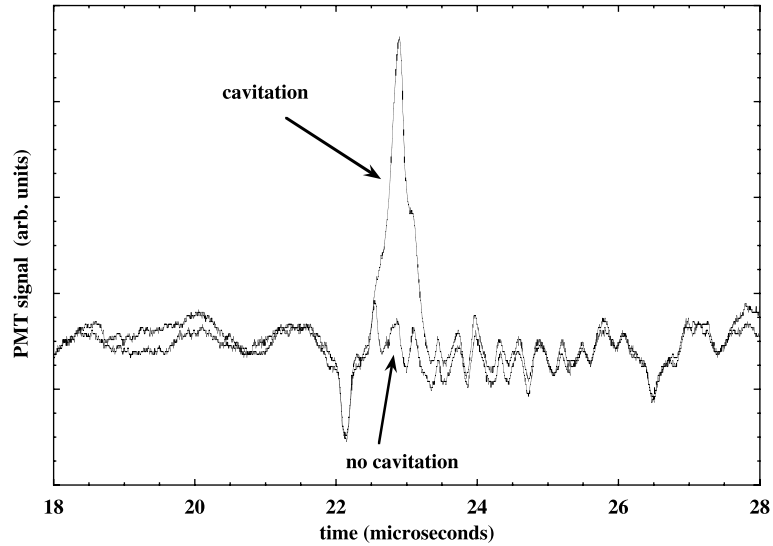


Fig. 16. For an excitation voltage +265 V on the outer side of the transducer (configuration D), a bubble appears at 22.5  $\mu$ s.

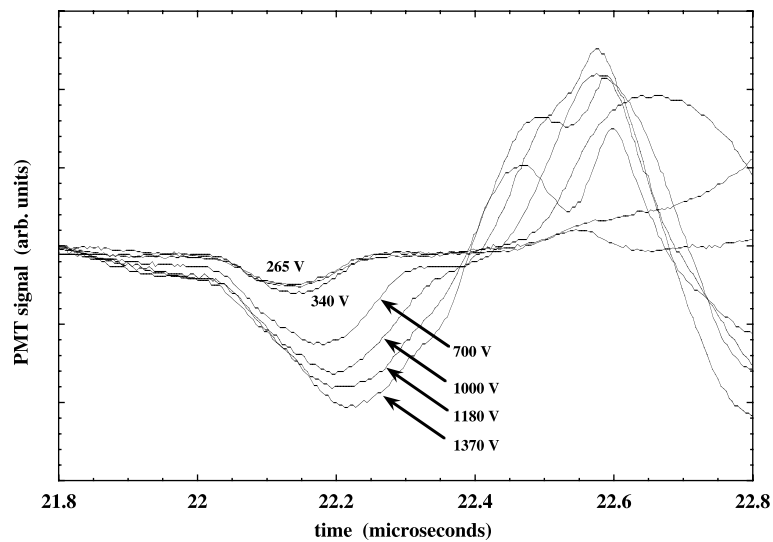


Fig. 17. Up to 1370 V, the acoustic signal continuously increases in the region corresponding to the first positive pressure swing (22–22.5  $\mu$ s) but no nucleation of any crystal is detected. After 22.5  $\mu$ s and at high voltage, the very large signals are due to cavitation.

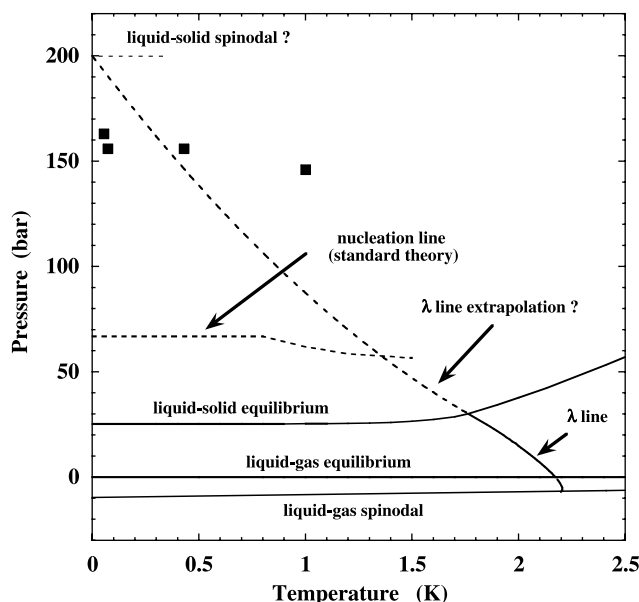


Fig. 18. The phase diagram extrapolated at high pressure. The broken line labelled "lambda line extrapolation?" is only a guess. The squares represent the maximum pressure reached in this experiment without nucleation of solid helium. Also represented are the well established spinodal line at negative pressure, and a possible liquid–solid spinodal limit at 200 bar.

The standard theory is indeed too simple. It writes the minimum work  $F(R)$  to form a spherical nucleus with radius  $R$  as

$$F(R) = 4\pi R^2 \gamma - \frac{4}{3}\pi R^3 \Delta P, \quad (6)$$

where  $\gamma = 0.17 \text{ erg/cm}^2$  is the liquid–solid interfacial tension<sup>19</sup> at the liquid–solid equilibrium pressure  $P_m$ ; as for  $\Delta P = (P_C - P_L)$ , it is the difference between the crystal pressure  $P_C$  inside the nucleus and the liquid pressure  $P_L$  outside (see Ref. 20).  $P_C$  is determined by the equality of chemical potentials inside and outside the nucleus. The difference  $\Delta P$  can be expressed as a departure from the equilibrium pressure  $P_m$  by expanding linearly the chemical potentials as a function of pressure. The following expression is obtained:

$$\Delta P = (P_C - P_L) = \frac{\rho_C - \rho_L}{\rho_L} (P_L - P_m). \quad (7)$$

Within these simple approximations, one finds a critical radius  $R_c = 2\gamma/\Delta P$  and an energy barrier

$$F(R_c) = \frac{16\pi\gamma^3}{3(\Delta P)^2}. \quad (8)$$

The nucleation rate is proportional to  $\exp[-F(R_c)/k_B T]$ .

This theory is too simple for three different reasons at least. First, a linear expansion of chemical potentials as a function of pressure is used, in other words compressibility is neglected, and this cannot be valid far away from the equilibrium pressure  $P_m$ . Second, when describing the cost in energy of a microscopic solid–liquid interface with a macroscopic quantity, the equilibrium interfacial tension  $\gamma$ , another questionable approximation is made. Furthermore,  $\gamma$  is taken as a pressure independent quantity, and this assumption has been particularly criticized by Maris and Caupin.<sup>21</sup> On the basis of their model, which accounts for a possible increase of  $\gamma$  as a function of pressure, and also for the compressibility of both phases, Maris and Caupin have found that the nucleation barrier should never be smaller than 200 K. If true, this would imply that the nucleation probability is negligible at any pressure on reasonable time scales, and that nucleation should never occur, except if there is an instability.

Such an instability was proposed by Schneider and Enz in 1971.<sup>7</sup> They noticed that the roton gap energy decreases with pressure, and they postulated that it might vanish at some critical pressure  $P_c$ . On approaching  $P_c$ , the rotons could become a soft mode with non-zero wavelength, so that liquid helium might spontaneously organize in a periodic state leading to crystalline order. We consider this possible instability as a liquid–solid spinodal limit where the response function of the liquid diverges at the roton wavelength, typically an interatomic distance. This liquid–solid instability is reminiscent of the dimple instability which occurs for a charged liquid surface when, as a result of increasing surface charge, a soft ripplon mode appears at a finite wavevector.<sup>22</sup> More recently, H.J. Maris used the density functional by Dalfovo *et al.*<sup>23</sup> to calculate  $P_c$ . He found about 200 bar,<sup>24</sup> a pressure at which the density is  $0.237 \text{ g/cm}^3$ , according to Eq. (3). As explained below, we should be able to improve our experimental method and to reach 200 bar or more, in order to see if this instability occurs.

Is it possible that nucleation occurred in our experiment but that we did not detect the nucleated crystals? We have assumed that, since the nucleated crystals were easy to detect in Chavanne’s experiment,<sup>2,3</sup> they should also be easy to detect in the present one. When calculating the energy barrier, one usually neglects dissipation (chemical potentials are

equal on both sides of the liquid–solid interface). However, after nucleation, when a macroscopic crystal grows in the overpressurized liquid, the growth velocity has to be limited by some dissipation mechanism. This has been extensively studied<sup>25</sup> for small departures from equilibrium: the simple relation

$$v = k \Delta\mu \quad (9)$$

links the growth velocity  $v$  to the driving force

$$\Delta\mu = \mu_L - \mu_C = \frac{\rho_C - \rho_L}{\rho_C \rho_L} (P - P_m), \quad (10)$$

where  $\mu$  is per unit mass,  $\rho_L$  is the liquid density and  $\rho_C$  the crystal density. The growth resistance  $k^{-1}$  is known to be very small in the low-temperature limit ( $k^{-1} \approx 3 \times T^4$  cm/s with  $T$  in Kelvin<sup>25</sup>). Chavanne *et al.* observed a growth velocity  $v$  of order 100 m/s for an overpressure  $P - P_m = 4.3$  bar. This was very fast, although not as fast as what one would extrapolate from Eq. (9). Of course, one does not expect crystals to grow faster than the speed of sound (366 m/s at the melting pressure), but still, when we applied 140 bar in this experiment, instead of 4.3 bar as in Chavanne's experiment, the crystals should grow even faster and be easier to detect. This is our main reason to believe that we have not detected crystals because they did not nucleate.

However, the fast growth rate of helium crystals is associated with the liquid being a superfluid. In particular, it seems necessary that the growth resistance has no contribution from viscous effects in the liquid which provides the necessary mass flow. We thus come to an interesting question: is liquid helium superfluid at 163 bar? The lambda line in stable liquid helium is known to have a negative slope  $dT_\lambda/dP$ . This is understood as a consequence of the density increase which makes the long-range quantum coherence due to particle exchange more and more difficult as the density increases.<sup>26</sup> It can also be calculated from the decrease of the roton gap as a function of pressure. In the metastable state at high pressure, the properties of liquid helium are nearly unknown but one can try to predict them. Caupin and Balibar<sup>27</sup> explained that the lambda line should meet the  $T = 0$  axis in the phase diagram at the instability pressure  $P_c$  where the roton gap vanishes. To calculate the pressure variation of the lambda line requires the use of a roton liquid theory whose parameters are unknown at high pressure, so that it has not yet been done, and one must rely on extrapolations with no rigorous justifications.

We have done the simplest possible extrapolation of the lambda line by using a second-order polynomial form, from the stable region to the ( $T = 0, P = 200$  bar) point. According to this, one expects a superfluid to

normal transition to occur around 190 bar at 50 mK (see Fig. 18). Even if we accounted for some adiabatic warming in the acoustic wave during compression, the temperature would keep below 100 mK at 163 bar and a superfluid to normal transition should not occur.<sup>28</sup> However, the lambda line in Fig. 18 is rather speculative, and we cannot exclude the possibility that superfluidity is destroyed during the largest positive pressure swings in our experiments, especially for our 1 K measurement. Normal liquid helium might even become very viscous, perhaps glassy. In such a case, the growth of crystals could become very slow and the nucleation of crystals impossible to observe because, in a fraction of a microsecond, these crystals would never grow to the micrometer size which is necessary for their detection. Now, if one reaches an instability at 200 bar, then a density change should be detectable with our technique even if the liquid is highly viscous. Once more, improvements of our experimental techniques are required in order to obtain some answers to these new questions.

## 5. CONCLUSION AND PERSPECTIVES

In this article, we have presented experimental results which lead to new theoretical questions. We have reached degrees of overpressurization in liquid helium which had never been achieved before by pressurizing liquid helium with ultrasound bursts during a fraction of a microsecond. We have found that, in such conditions, nucleation of solid helium does not occur in liquid helium up to 163 bar, far beyond the nucleation threshold predicted by the standard theory of homogeneous nucleation. We have explained why this standard theory is too simple for any accurate prediction so that much more elaborate theories are needed. Our results lead to new questions which concern the pressure dependence of the liquid-solid interfacial tension, the possible existence of a liquid-solid instability at 200 bar and the shape of the superfluid transition line in the metastable region of the phase diagram, at high pressure.

In the future, we plan to change our hemispherical transducer for a spherical one. This can easily be done by gluing two hemispheres facing each other. The previous experiments by Chavanne *et al.* in a quasi-spherical geometry<sup>2,3</sup> have shown that spherical waves are highly non-linear so that their positive swings are very large compared to their negative ones. These effects would allow us to reach larger overpressures without triggering cavitation during the previous negative swing of the wave. The output power of our present amplifiers seems largely sufficient to detect the homogeneous nucleation of helium crystals if it occurs near an instability line around 200 bar. For this future series of experiments, we anticipate problems of calibration of the wave amplitude and the nucleation

threshold pressure. We hope to do this by improving the numerical simulation of the focusing of large amplitude sound waves which we have started in collaboration with C. Appert *et al.*<sup>15</sup>

### ACKNOWLEDGMENTS

We are grateful to H.J. Maris and D.M. Ceperley for many fruitful discussions.

### REFERENCES

1. S. Balibar, T. Mizusaki, and Y. Sasaki, *J. Low Temp. Phys.* **120**, 293 (2000).
2. X. Chavanne, S. Balibar, and F. Caupin, *Phys. Rev. Lett.* **86**, 5506 (2001).
3. X. Chavanne, S. Balibar, and F. Caupin, *J. Low Temp. Phys.* **125**, 155 (2001).
4. F. Caupin and S. Balibar, *Phys. Rev. B* **64**, 064507 (2001).
5. S. Balibar, B. Castaing and C. Laroche, *J. Phys. (Paris) Lett.* **41**, 283 (1980); V.L. Tsymbalenko, *J. Low Temp. Phys.* **88**, 55 (19); J.P. Ruutu, P.J. Hakonen, J.S. Penttila, A. V. Babkin, J. P. Saramaki and E. B. Sonin, *Phys. Rev. Lett.* **77**, 2514 (1996); Y. Sasaki and T. Mizusaki, *J. Low Temp. Phys.* **110**, 491 (1998); T. A. Johnson and C. Elbaum, *Phys. Rev. E* **62**, 975 (2000).
6. F. Caupin, S. Balibar, and H. J. Maris, *Physica B* **329–333**, 356 (2003).
7. T. Schneider and C. P. Enz, *Phys. Rev. Lett.* **27**, 1186 (1971).
8. J. Nissen, E. Bodegom, L. C. Brodie, and J. S. Semura, *Phys. Rev. B* **40**, 6617 (1989).
9. S. Balibar, X. Chavanne and F. Caupin, *Physica B* **329–333**, 380 (2003).
10. K. O. Keshishev, A. Ya. Parshin and A. V. Babkin, *Zh. Eksp. Teor. Fiz.* **80**, 716 (1981) [*Sov. Phys. JETP* **53**, 362 (1981)].
11. J. Bodensohn, K. Nicolai, and P. Leiderer, *Z. Phys. B* **64**, 55 (1986).
12. S. Balibar, H. Alles and A. Ya. Parshin, submitted to *Rev. Modern Phys.* (2004).
13. L. Darrasse, *Rev. Sci. Instrum.* **53**, 1561 (1982).
14. X. Chavanne, S. Balibar, F. Caupin, C. Appert, and D. d’Humières, *J. Low Temp. Phys.* **126**, 643 (2002).
15. C. Appert, C. Tenaud, X. Chavanne, S. Balibar, F. Caupin, and D. d’Humières, *Eur. Phys. J. B* **35**, 531 (2003).
16. In Ref. 4, the inertia of the transducer was neglected so that no phase shift was predicted between the excitation voltage and the transducer response. Here, we find a ( $\pi/2$ ) phase shift. We are grateful to H. J. Maris who first mentioned this former mistake to us.
17. H. J. Maris, *Phys. Rev. Lett.* **66**, 45 (1991).
18. B. Abraham, Y. Eckstein, J. B. Ketterson, M. Kuchnir, and P. R. Roach, *Phys. Rev. A* **1**, 250 (1970).
19. D. O. Edwards, M. S. Pettersen, and H. Baddar, in *Excitations in 2D and 3D Quantum Fluids*, eds. A. F. G. Wyatt and H. J. Lauter (Plenum Press, New York, 1991), p.361.
20. L. D. Landau and E. M. Lifshitz, *Course of Theoretical Physics, Vol. 5, Statistical Physics* (Pergamon press, Oxford, 1980), p. 533.
21. H. J. Maris and F. Caupin, *J. Low Temp. Phys.* **131**, 145 (2003).
22. P. Leiderer, *J. Low Temp. Phys.* **87**, 247 (1992).
23. F. Dalfovo, A. Latri, L. Pricapenko, S. Stringari, and J. Treiner, *Phys. Rev. B* **52**, 1193 (1995).
24. H. J. Maris, private communication, unpublished.
25. K. O. Keshishev, A. Ya. Parshin, and A. V. Babkin, *Pis'ma Zh. Eksp. Teor. Fiz* **30**, 63 (1979) [*Sov. Phys. JETP Lett.* **30**, 56 (1979)]; R. M. Bowley and D. O. Edwards, *J. Physique (France)* **44**, 723 (1983); E. Rolley, C. Guthmann, E. Chevalier, and S. Balibar, *J. Low Temp. Phys.* **99**, 851 (1995).

26. G. H. Bauer, D. M. Ceperley, and N. Goldenfeld, *Phys. Rev. B* **61**, 9055 (2000).
27. F. Caupin and S. Balibar, in *Liquids Under Negative Pressure*, eds., A. R. Imre *et al.* (Kluwer Academic Publishers, 2002), p. 201.
28. We have looked for some evidence of the liquid undergoing a superfluid to normal transition at high pressure and low temperature. A change in compressibility at such a transition could show up as some distortion in the shape of the acoustic wave, consequently in the signal from the light scattering by the sound pulse. We have not found convincing evidence that such a distortion occurs at any well defined amplitude of the wave.
29. H. J. Maris, private communication (2004).